Supporting information for

Triplet Dynamic Nuclear Polarization of Pyruvate via Supramolecular Chemistry

Tomoyuki Hamachi,[a] Koki Nishimura,[a] Keita Sakamoto,[a] Yusuke Kawashima,[a] Hironori Kouno,[a] Shunsuke Sato[c], Go Watanabe[c,d], Kenichiro Tateishi,[e,f] Tomohiro Uesaka,[e,f] Nobuhiro Yanai*[a,b,g]

a. Department of Applied Chemistry, Graduate School of Engineering, Kyushu University, 744 Moto-oka, Nishi-ku, Fukuoka 819-0395, Japan.

E-mail: yanai@mail.cstm.kyushu-u.ac.jp

b. Center for Molecular Systems (CMS), 744 Moto-oka, Nishi-ku, Fukuoka 819-0395, Japan.

c. Department of Physics, School of Science, Kitasato University, Sagamihara, Kanagawa 252-0373, Japan.

d. Kanagawa Institute of Industrial Science and Technology (KISTEC), 705-1 Shimoizumi, Ebina, Kanagawa 243-0435, Japan.

e. Cluster for Pioneering Research, RIKEN, 2-1 Hirosawa, Wako, Saitama 351-0198, Japan.

f. RIKEN Nishina Center for Accelerator-Based Science, 2-1 Hirosawa, Wako, Saitama 351-0198, Japan.

g. PRESTO and FOREST, JST, Honcho 4-1-8, Kawaguchi, Saitama 332-0012, Japan.

Materials and Methods

Materials

All reagents and solvents for measurements were used as received without further purification. Glycerol, sodium hydroxide and sodium bicarbonate were purchased from Kishida chemilcal. β-cyclodextrin was purchased from Wako Pure Chemical. Sodium pyruvate, [1-^{13}C, d_3] pyruvic acid, deuterium oxide and glycerol-d_8 were purchased from Sigma Aldrich. Deionized water was generated by Direct-Q UV (Merck Millipore). Analytical grade methanol, ethanol, acetone and were purchased from Wako Pure Chemicals. The synthesis and characterization of H_2PDBA have been reported in our previous work (*1*). Sodium salts of H_2PDBA (NaPDBA) was prepared by neutralizing H_2PDBA with NaOH methanol solution and the solvent was removed. 1 mM of NaPDBA, 5 mM of βCD and 1.5 M of NaPyr in DNP juice was prepared by dissolving NaPyr into DNP juice ([NaPDBA] = 1 mM and [βCD] = 5 mM) and sonicated for 5 mins to disperse NaPyr completely. [1-^{13}C, d_3] NaPyr was prepared by dissolving 160 μL of [1-^{13}C, d_4] Pyruvic acid into 1 M of sodium bicarbonate in deuterium oxide. 25 mL of ethanol was slowly added to recrystallize [1-^{13}C, d_3] NaPyr. Obtained [1-^{13}C, d_3] NaPyr was washed by 20 mL of acetone.

General characterizations

UV-vis absorption spectra were measured by JASCO V-670 and V-770 spectrophotometers. ^{1}H NMR (400 MHz) spectra were measured on a Bruker Ascend NMR 400 MHz.

Time-resolved ESR

Time-resolved ESR measurement was conducted on a home-built spectrometer (Fig. S1) which has been described in our previous report (*2*).

The samples were inserted into the dielectric resonator inside of an electromagnet (MC160-60G-0.8T, Takano Original Magnet) which is controlled by a function generator (33500B, Keysight). The sample was photo-excited by using a pulsed laser (Tolar-527, Beamtech Optronics). The pulse width, maximum repetition rate and maximum power of this laser are 200 ns, 5 kHz and 400 W, respectively. For samples, the repetition rate and the power of the laser were set to 100 Hz and 0.3 W.

A microwave was generated with the power of ~1 mW (SG24000H, DS Instruments) and amplified by using a power amplifier (ALN0905-12-3010, WENTEQ Microwave Corp), then converted to DC with a diode detector (DHM185AB, Herotek). ESR signal was also amplified and the noise was cut off by using two amplifiers (SA-230F5, NF ELECTRONIC INSTRUMENTS and 5305 differential amplifiers, NF ELECTRONIC INSTRUMENTS). The ESR signal was detected by an oscilloscope (DSOX3024T, Keysight). The temperature was controlled by flowing cold nitrogen gas into the microwave cavity.

The dielectric resonator was fabricated as shown in Fig. S2. A ring-shaped dielectric ceramic (M29, MARUWA) with an outer diameter of 6.8 mm, an inner diameter of 2.1 mm, and a thickness of 2.5 mm was used. The hole with diameter of 14 mm was made on the copper blocks and closed by two copper clad laminate (CCL) boards to insert the

dielectric ceramic. There is a hole with diameter of 2.1 mm on the top side CCL boards to insert the sample, and there are three holes on the center of front, back and side of copper blocks for microwave irradiation, laser irradiation and flowing the gas for temperature control with diameter of 8 mm, 6 mm and 5 mm, respectively. Two dielectric ceramics were hold by PTFE in the center of resonator. The waveguide was attached to the front of the resonator and a small copper plate, placed between the waveguide and the resonator, was controlled by a PTFE screw to adjust the microwave reflectivity. The resonance frequency of the fabricated cavity resonator was 9 GHz.

ESR spectra were analyzed in MATLAB version R2019b Update 8 (The Mathworks, Inc.). The fitting parameters are summarized in Table S1 and S2.

DNP and RAMP-CP experiment

DNP experiment was carried out on a home-built spectrometer (Fig. S3), which has been described in our previous report (*2*). It consists of electromagnet (MC160-60G-0.8T, Takano Original Magnet), microwave resonator, coil for magnetic field sweep and pulsed laser. The sequence control and NMR signal detection were performed by OPENCORE NMR spectrometer (*3*).

The cavity was fabricated as shown in Fig. S4. The hole with diameter of 21.5 mm was made on the copper blocks and closed by two CCL boards to adjust the resonant frequency of Ku-band. There is a hole with diameter of 5 mm on the top side CCL boards to insert the samples, and there are three holes on the center of front, back and side of copper blocks for microwave irradiation, laser irradiation and flow of cold nitrogen gas to kept the sample temperature, with diameter of 7 mm, 6 mm and 5 mm, respectively. The microwave reflectivity was adjusted by a Teflon screw as with time-resolved ESR setup. the resonance frequency of the fabricated cavity resonator was about 17.3 GHz. 1-turn saddle coil, four enamel wires which were connected to each other, were inserted into the resonator to surround the sample. An induced magnetic field was applied to the sample by a current flowing in the copper wire, and the induced field direction is parallel to the static magnetic field. The magnetic field was swept from a high field to a low field over a few tens of microseconds. The coils for the NMR detection were installed on the top of the resonator. The coil was made by winding enameled wire. The oscillating magnetic field from the coil and the static magnetic field from the electromagnet were arranged perpendicular to each other.

The sample was photo-excited by using pulsed laser (Tolar-527, Beamtech Optronics) and kept the temperature by flowing cold nitrogen gas, same as time-resolved ESR setup. For triplet-DNP experiments, the repetition rate and the power of the laser were set to 500 Hz and 2.7 W. The continuous microwave was generated (SG24000H, DS Instruments) and converted to a pulsed wave using a pin diode (S1517D, L3HARRIS). The pulsed wave was amplified by using a power amplifier (AMP4081P-CTL, EXODUS ADVANCED COMMUNICATIONS) and sent into the resonator by a coaxial cable with the transmission loss of ~1dB. The magnetic field sweep was performed by applying an amplified triangular wave to a copper wire built in the resonator (Fig. S4). The source triangular wave was generated from function generator (WF1974, NF ELECTRONIC INSTRUMENTS). This triangular wave was amplified tenfold using an operational amplifier (137-PA05, Apex

Microtechnology) and applied to the copper wire to reach a maximum of ±50 V. NMR signals were obtained by OPENCORE NMR spectrometer. The solenoid coil was used as NMR probe coil and mounted on the top of resonator (Fig. S4). The sample was rifted up to the probe coil by using stepping motor within 1 s before NMR detection. In the case of protons in solid samples, a magic echo sequence was used because the short T_2 relaxation time and strong dipole interaction make it difficult to detect them with ordinary single pulses or spin echoes.

Polarization transfer from ^{1}H spins to ^{13}C spins was performed by a using a ramped amplitude cross-polarization (RAMP-CP) sequence. To perform double resonance, a split coil was placed across the solenoid coil for detection (Fig. S4). RAMP-CP was performed by irradiating radio waves with 20 kHz field on ^{13}C channels from the solenoid coil while irradiating radio waves with field sweep from 15 kHz to 25 kHz on ^{1}H channels from the split coil for 10 ms.

Molecular dynamics simulation

All-atom MD simulations in this study were performed by using the MD program GROMACS 2020.5. In the initial structure of the system of NaPDBA-βCD complex ([NaPDBA] = 1 mM and [βCD] = 5 mM) in glycerol/water (6/4, v/v), the complexes of NaPDBA with βCD were assembled close to each other and solvents and isolated βCD molecules were placed in the surrounding space to fill the cubic MD cell. The numbers of molecules were 4 for NaPDBA, 20 for βCD, 29050 for glycerol, and 78672 for water molecules. For the system of NaPDBA-βCD complex in the presence of NaPyr ([NaPDBA] = 1 mM, [βCD] = 5 mM, and [NaPyr] = 1.5 M) in glycerol/water (6/4, v/v), the assembly of NaPDBA-βCD complexes was also placed in the center of the MD cell and NaPyr molecules were randomly inserted into the solvents. The numbers of molecules were 4 for NaPDBA, 20 for βCD, 6000 for NaPyr, 25650 for glycerol, and 69498 for water molecules. The generalized Amber force field (*4*) parameters were used for the force field parameters of NaPDBA, βCD, NaPyr, and glycerol and the TIP4P-Ew (*5*) model was used for the water molecules. As NaPDBA and NaPyr are composed of sodium ion and $PDBA^{-}$ and Pyr^{-}, respectively, their partial atomic charges were separately assigned. The atomic charges of PDBA–, Pyr^{-}, βCD, and γCD were calculated using the restrained electrostatic potential (RESP) (*6*) methodology, based on DFT calculations (B3LYP/6-31G(d,p)) using the GAUSSIAN 16 revision C01 program (Gaussian, Inc., Wallingford CT, 2016).

In the present MD simulations, pre-equilibration and equilibration runs at room temperature (300 K) were sequentially carried out after the steepest energy minimization. During the 5 ns pre-equilibration, the temperature and pressure of the system were kept constant using Berendsen thermostat and barostat (*7*) with the relaxation times of 0.2 and 2.0 ps, respectively. The equilibration was run for 20 ns using the Nosé-Hoover thermostat (*8*) and Parrinello-Rahman barostat (*9*) with the relaxation times of 1.0 and 5.0 ps, respectively. The pressure of the system for all MD simulations was kept at 1 bar. All bonds connected to hydrogen atoms were constrained with LINCS (*10*) algorithm. The time step of both pre-equilibration and equilibration was set to 2 fs. The long-range Coulomb interactions were calculated with the smooth particle-mesh Ewald method (*11*) with a grid

spacing of 0.30 nm. The real space cutoff for both Coulomb and van der Waals interactions was 1.2 nm.

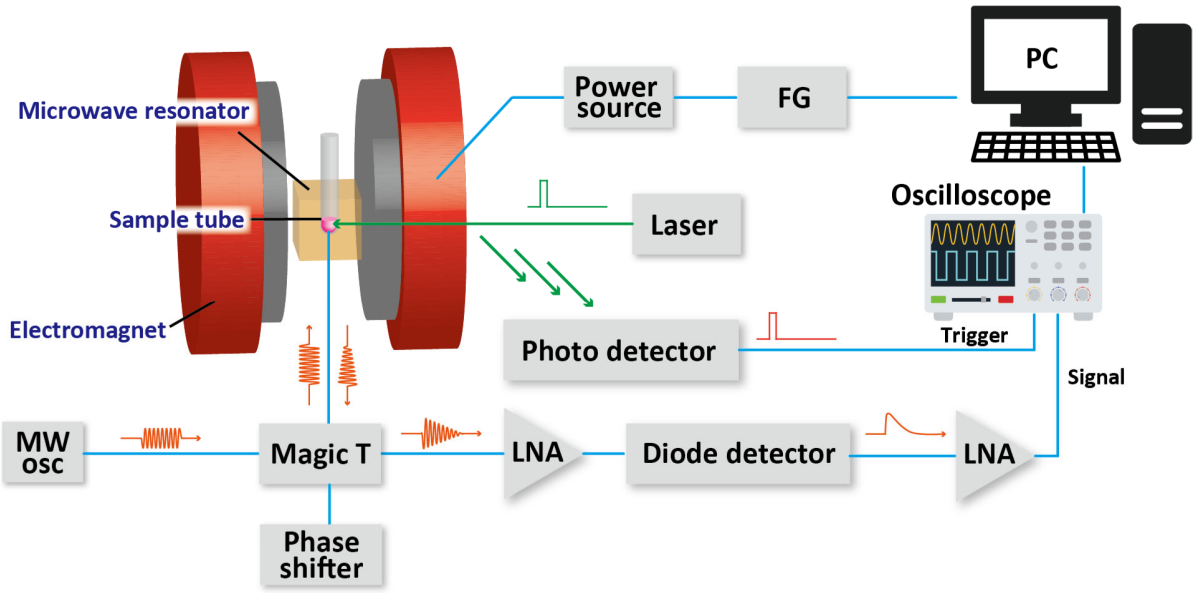

Fig. S1 Setup for time-resolved ESR. LNA: low noise amplifier; MW osc: microwave oscillator; FG: function generator.

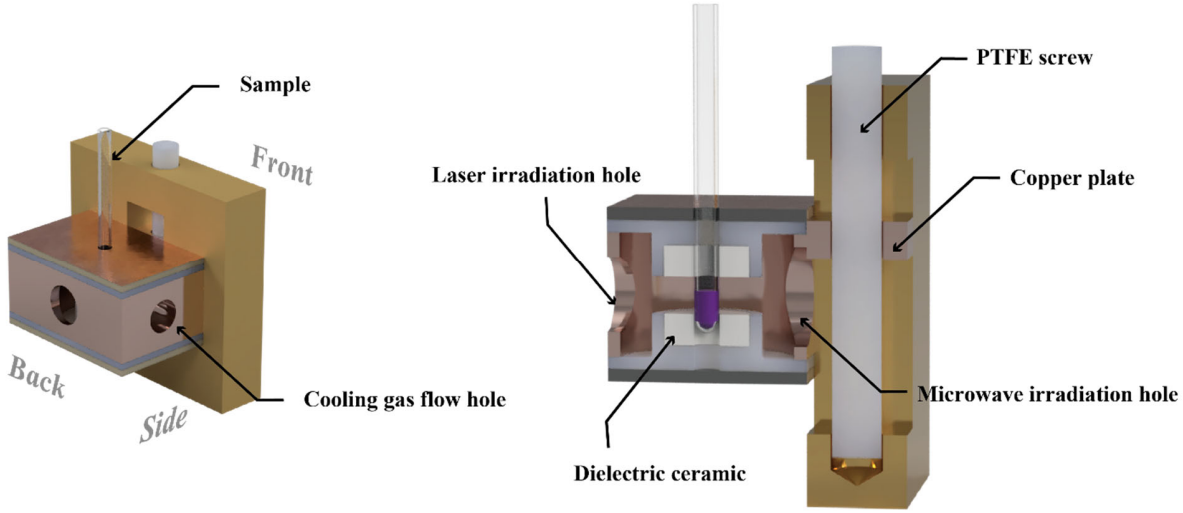

Fig. S2 The cavity resonator in the time-resolved ESR setup. Overall view (left) and cross-sectional view (right).

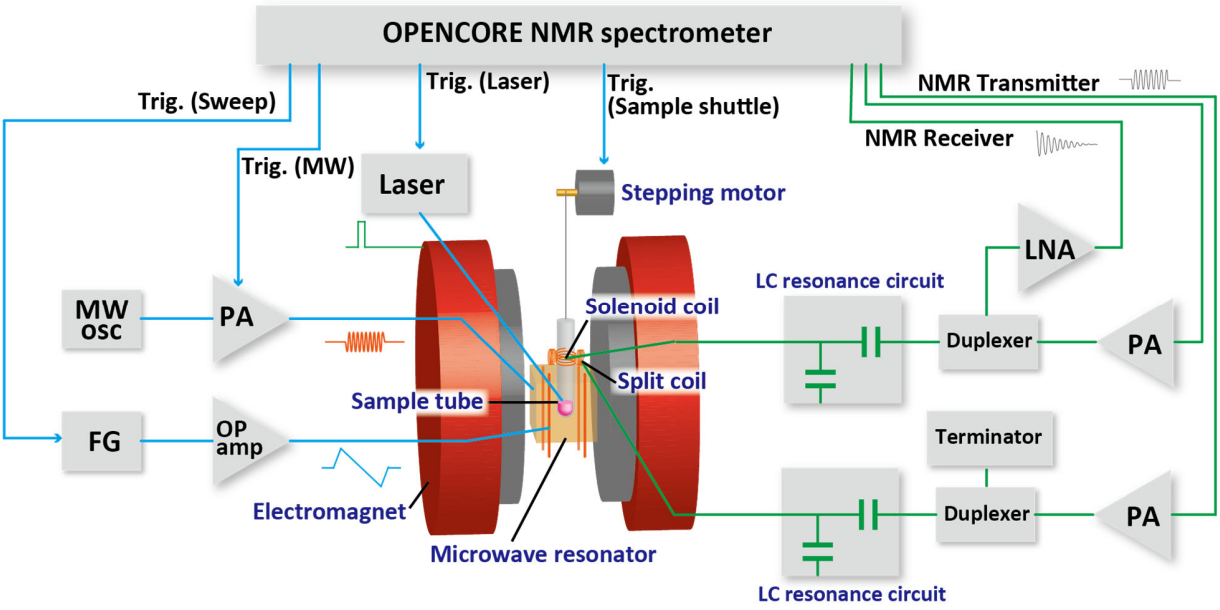

Fig. S3 Setup for triplet-DNP. PA: power amplifier; MW osc: microwave oscillator; FG: function generator; Trig.: TTL trigger signal; LNA: low noise amplifier.

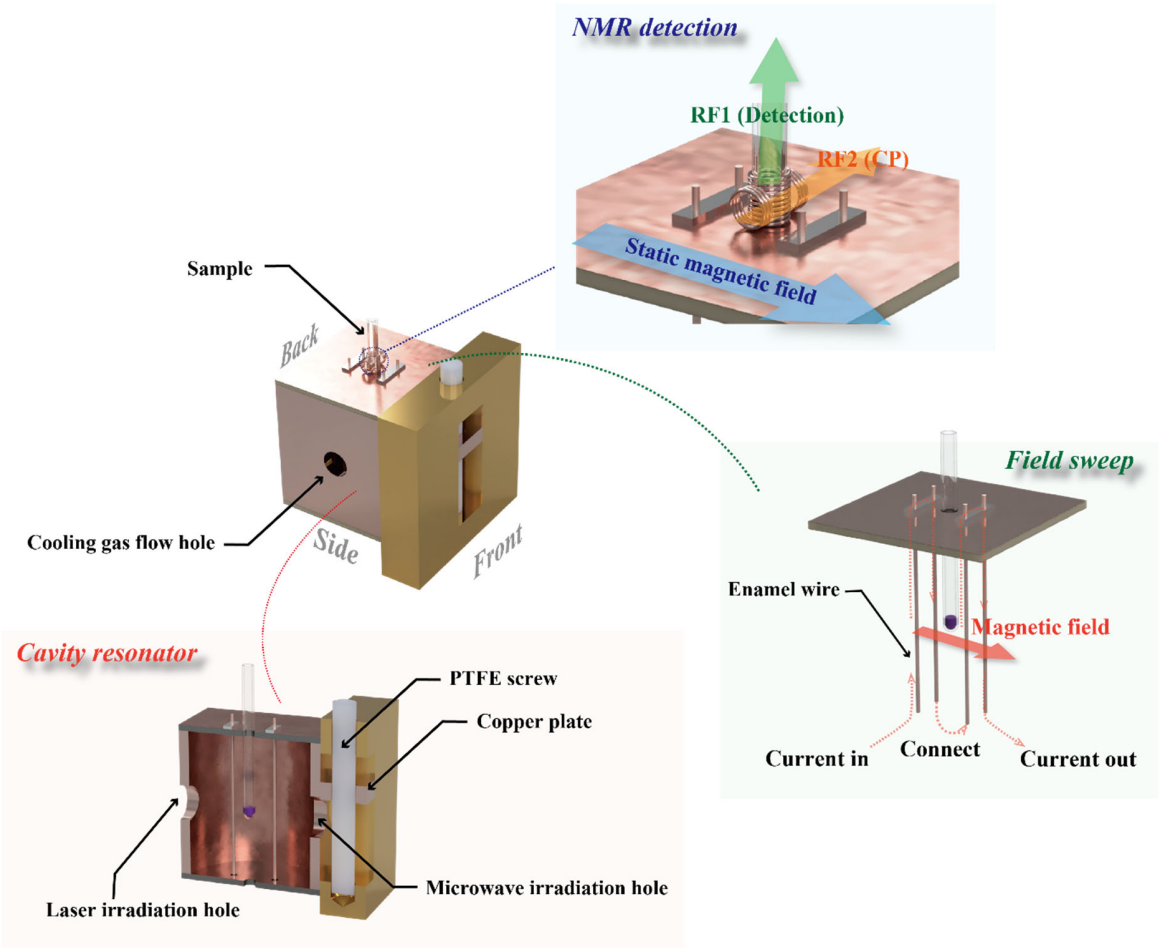

Fig. S4 The resonator used in triplet-DNP. NMR detection part (blue), field sweep part (green) and cavity resonator (red).

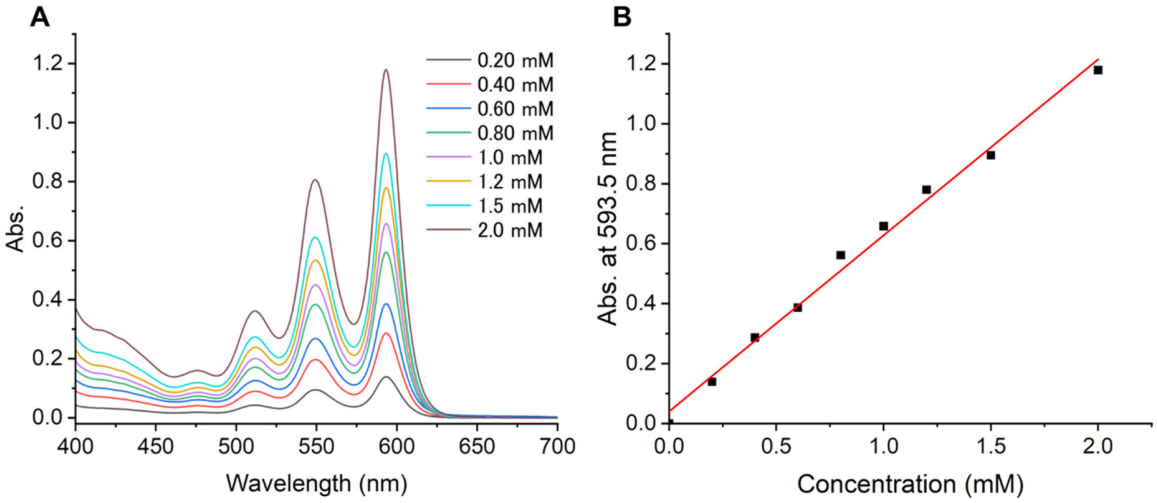

Fig. S5 (A) Concentration-dependent absorption spectra of NaPDBA in methanol. (B) Lambert-Beer plot of NaPDBA in methanol at 593.5 nm. The fitting results is shown as a red line according to be following equation, $y = Ax+B$. The observed linearity supports the molecularly-dispersed state of NaPDBA in methanol at room temperature.

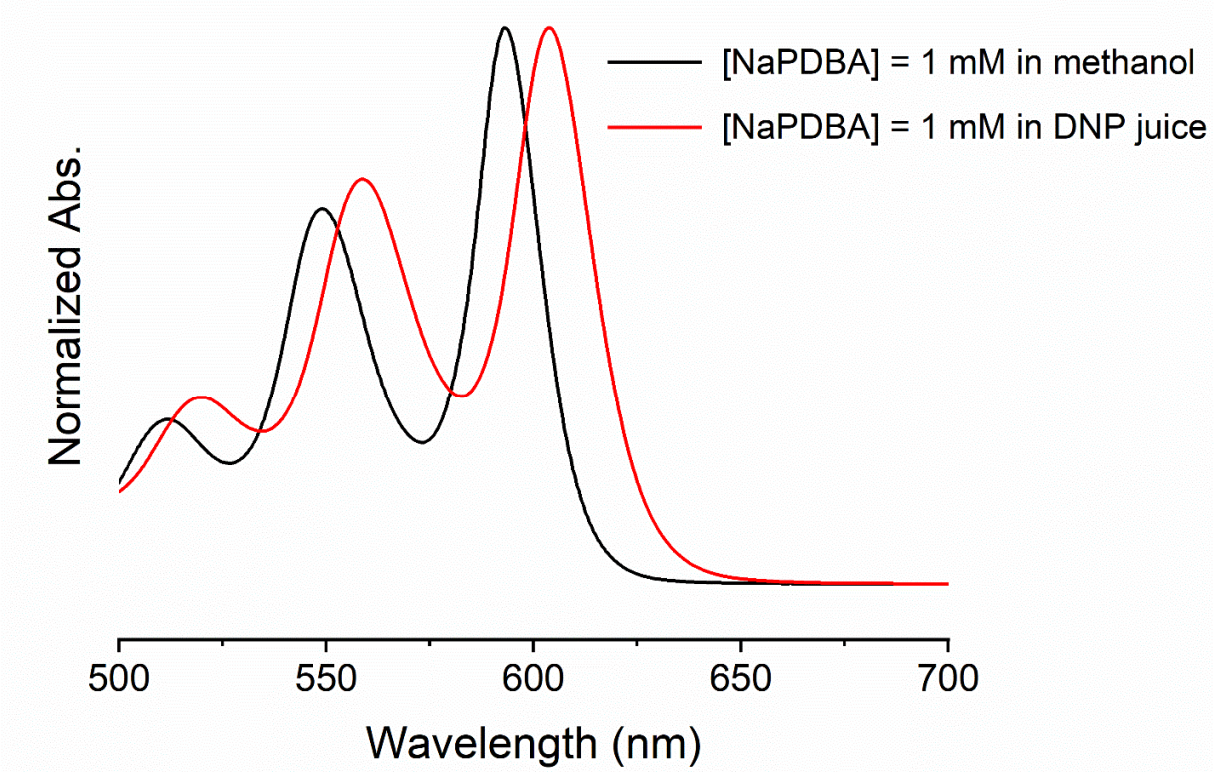

Fig. S6 Absorption spectra of NaPDBA ([NaPDBA] =1 mM) in methanol and DNP juice. The absorption peak tops are 593.5 nm and 604 nm in methanol and DNP juice, respectively.

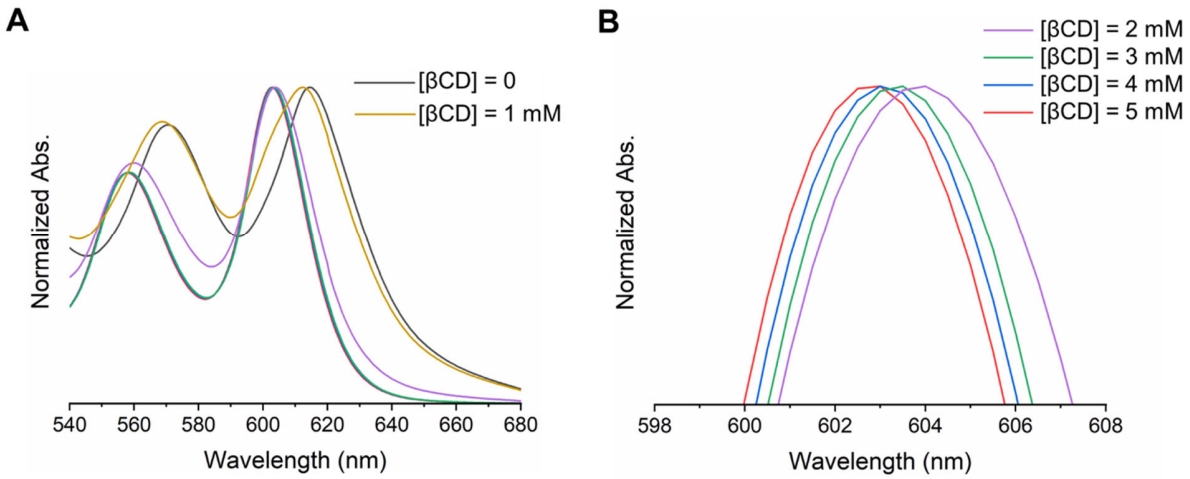

Fig. S7 (A) Absorption spectra of 1 mM of NaPDBA in DNP juice containing 1.5 M of NaPyr and different concentration of βCD. (B) Zoomed-in absorption spectra for different βCD concentrations from 2 mM to 5 mM.

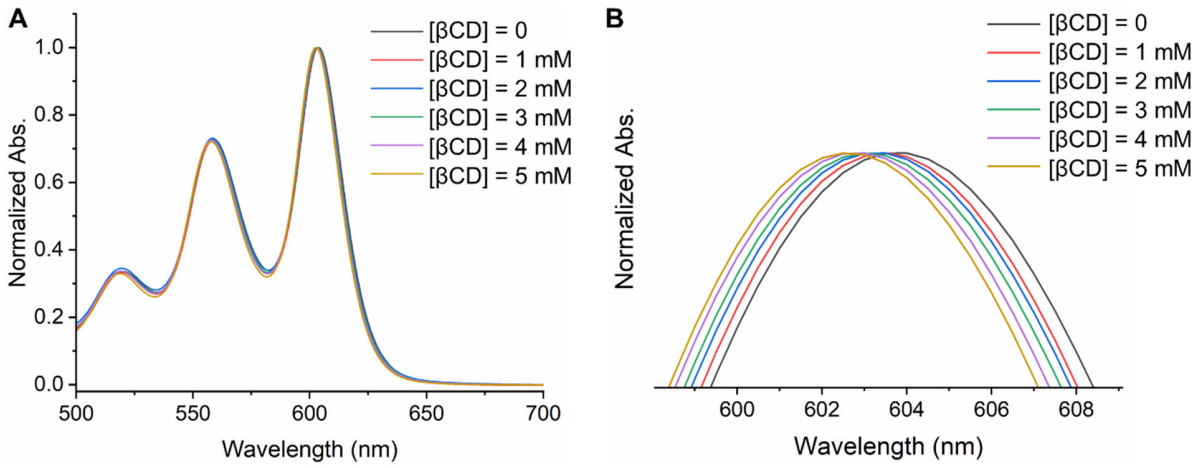

Fig. S8 (A) Absorption spectra of 1 mM of NaPDBA in DNP juice containing different concentration of βCD without NaPyr. (B) Zoomed-in absorption spectra for different βCD concentrations.

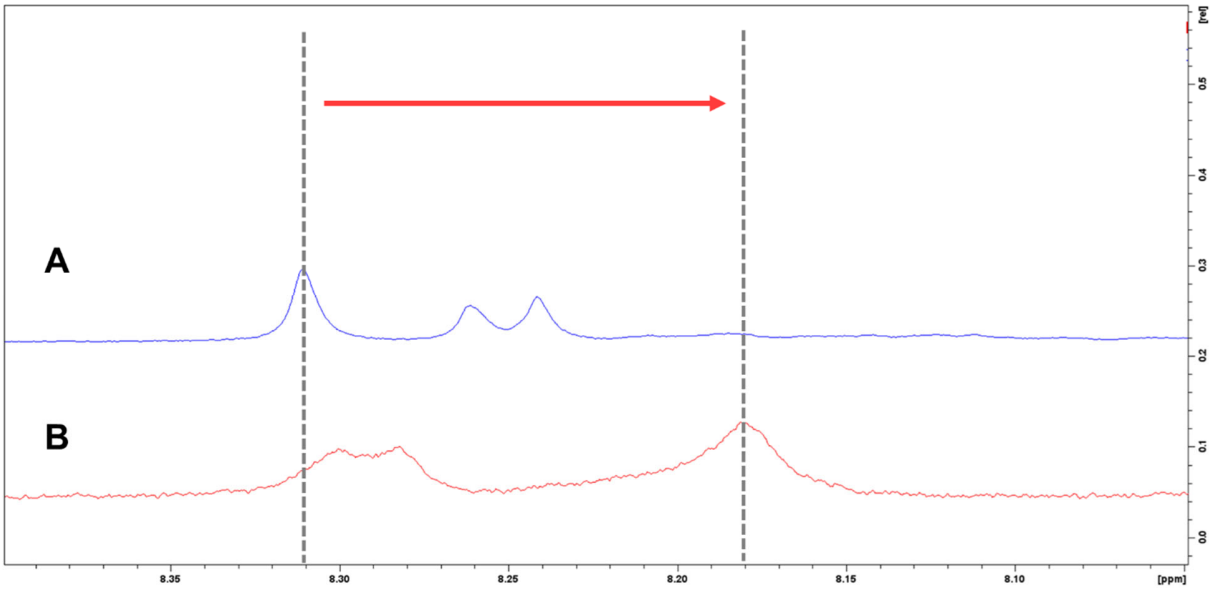

Fig. S9 (A) ^{1}H NMR spectrum of NaPDBA ([NaPDBA] = 1 mM) in glycerol-d_8/D_2O (6/4, v/v) at room temperature. (B) ^{1}H NMR spectrum of NaPDBA, βCD and NaPyr-d_3 ([NaPDBA] = 1 mM, [βCD] = 5 mM and [NaPyr-d_3] = 1.5 M) in glycerol-d_8/D_2O (6/4, v/v) at room temperature. The residual glycerol ^{1}H peak was used as the internal standard.

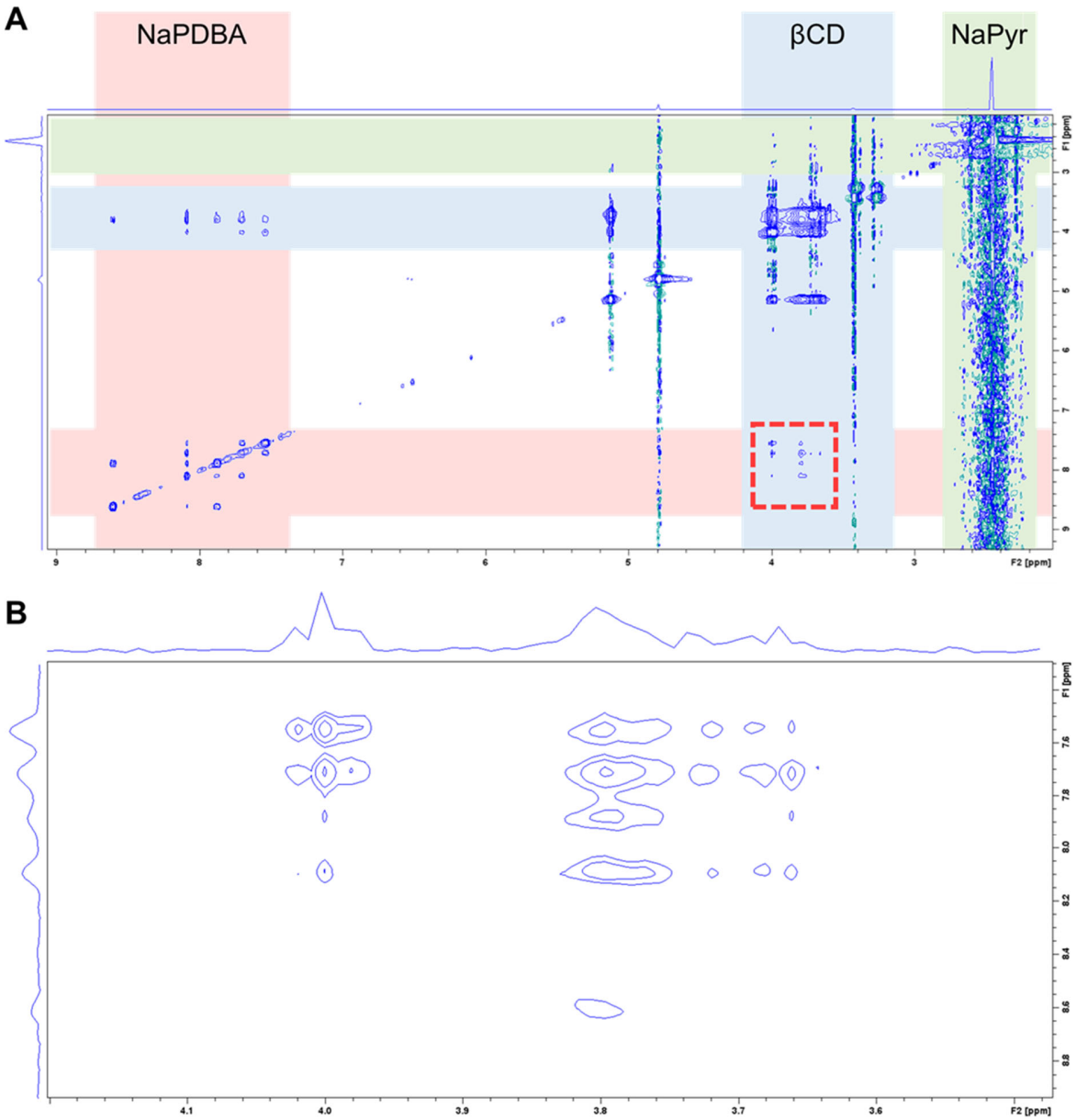

Fig. S10 (A) 2D NOESY spectra of NaPDBA, βCD and NaPyr ([NaPDBA] = 1 mM, [βCD] = 5 mM and [NaPyr] = 1.5 M) in D_2O at room temperature. (B) Enlarged view of the red dotted line in Fig. S10A. The residual water peak was used as the internal standard.

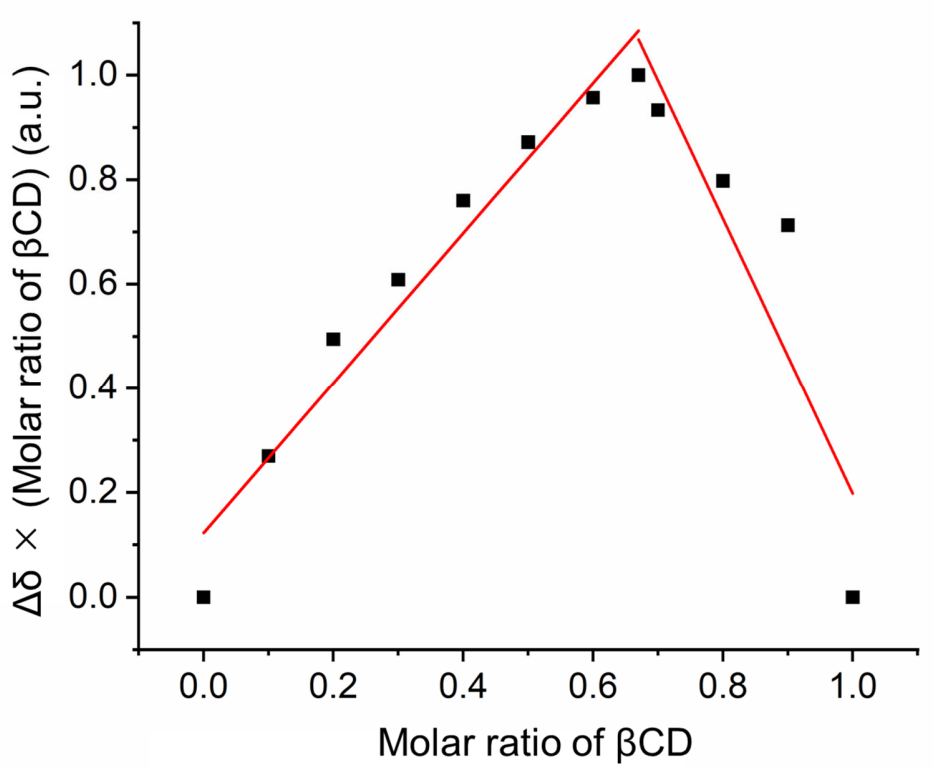

Fig. S11 Job plot of NaPDBA and βCD in D_2O containing NaPyr. The total concentration of NaPDBA and βCD was kept as 2 mM and the concentration of NaPyr was kept as 1.5 M. The chemical shift difference (Δδ) of the peak at around 3.96 ppm is shown. The residual water peak was used as the internal standard.

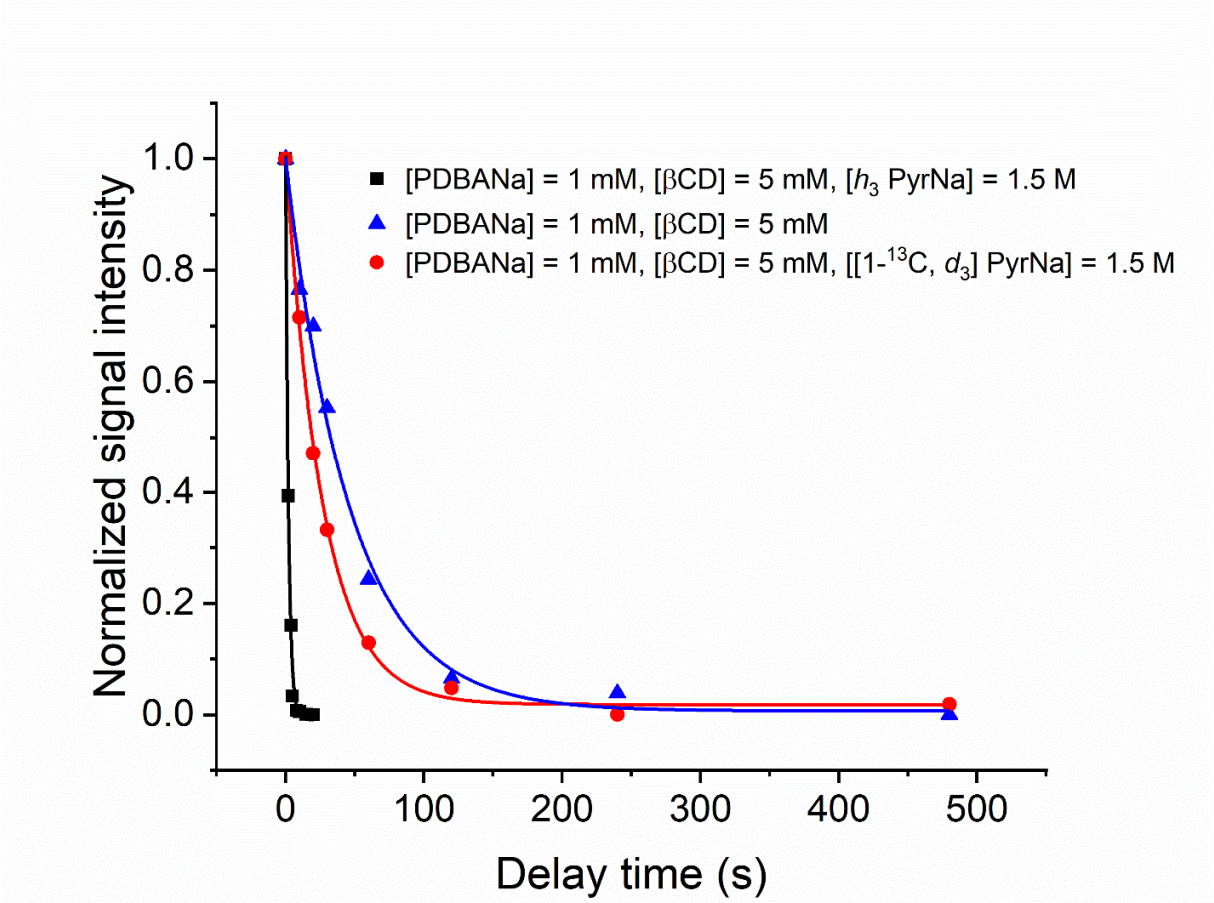

Fig. S12 ^{1}H NMR signal decays of NaPDBA-βCD with h_3-NaPyr (black dots), without NaPyr (blue dots), and with 1.5 M d_3-NaPyr (red dots) in DNP juice obtained by changing the interval from triplet-DNP to NMR measurements at 100 K. Single exponential fitting of each data gave T_1 values of 2 s (black), 26 s (red) and 46 s (blue), respectively.

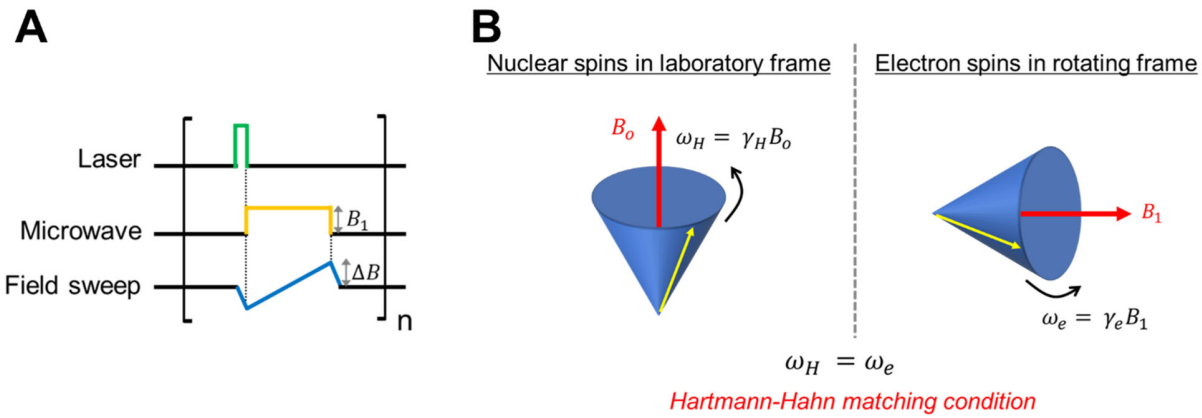

Fig. S13 (A) Integrated Solid Effect (ISE) sequence. (B) Hartmann-Hahn matching condition. Following the laser irradiation to produce the spin polarized triplet electrons, microwave and magnetic field sweep are applied simultaneously (Fig. S13A). The spin polarization of electron spins can be transferred to nuclear spins (^{1}H spins in this experiment) by matching the Rabi frequency of electron spins and the Larmor frequency of nuclear spins under the microwave irradiation (Fig. S13B) (*12-15*). This condition is called as Hartmann-Hahn condition; $\gamma_e B_1 = \gamma_H B_0$, where γ_e, γ_H is the gyromagnetic ratio of the electron and proton spin, respectively, B_0 is the external magnetic field, and B_1 is the oscillating magnetic field by microwave irradiation. However, not all electron spins can be employed for polarization transfer at one time since the ESR spectra of electron spins are broadened by hyperfine interactions and random orientation of polarizing agents. In order to use a larger number of electron spins for polarization transfer, the magnetic field is swept during microwave irradiation. Spin polarization diffuses throughout the solid sample due to magnetic dipolar interactions between ^{1}H spins. Repeating the ISE sequence builds up ^{1}H spin polarization, which is saturated by spin-lattice relaxation.

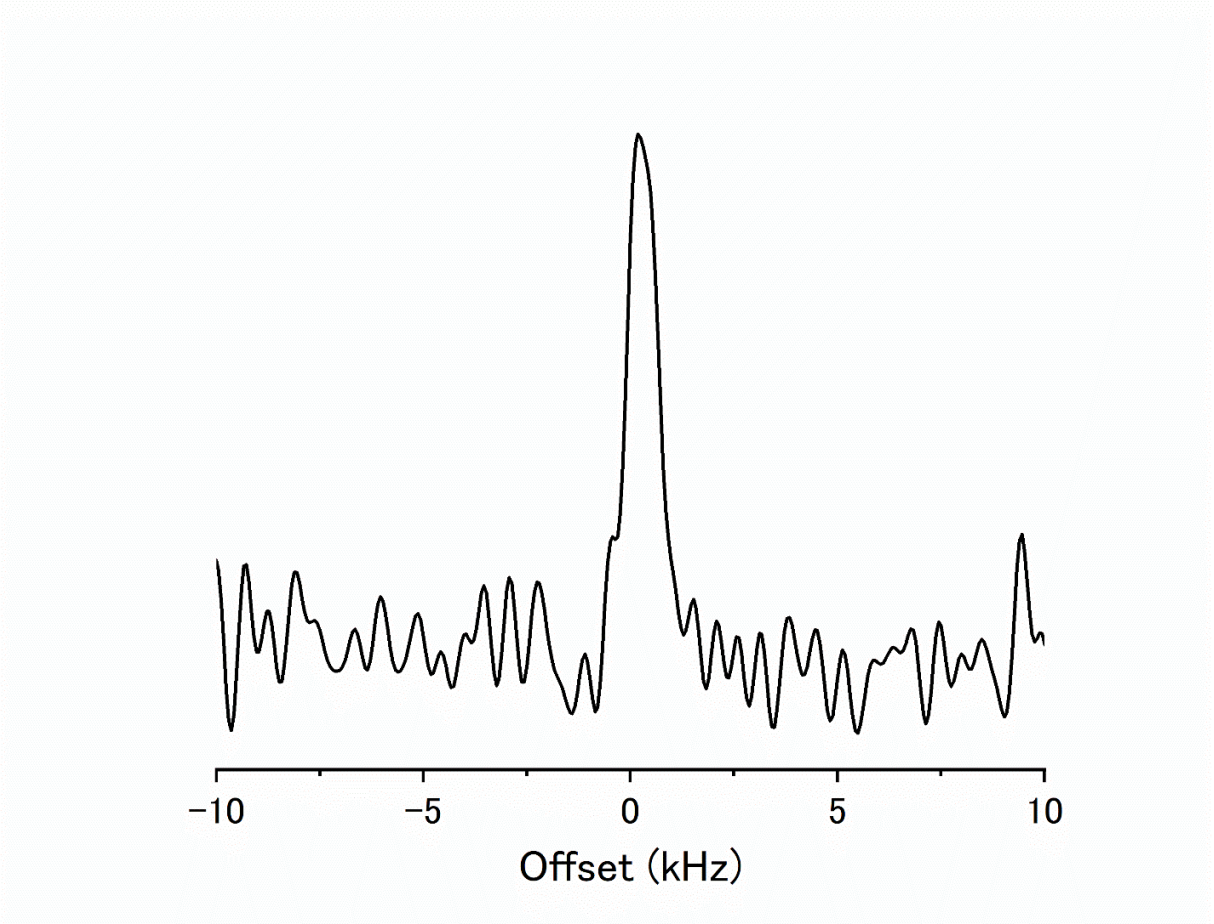

Fig. S14 ^{13}C NMR of ^{13}C-methanol. Spectra were accumulated 500 times with a 5 minutes delay in a 0.67 T magnetic field (6.864 MHz).

Table S1. Zero-field splitting parameters and relative zero-field populations derived from the simulation of the time-resolved ESR spectra of NaPDBA-βCD complex in DNP juice with and without NaPyr at 140 K shown in Fig. 4A.

Sample	D (MHz)	E (MHz)	p_x	p_y	p_z
[NaPDBA] = 1 mM, [βCD] = 5 mM	1335	-45	0.7	0.25	0.05
[NaPDBA] = 1 mM, [βCD] = 5 mM, [NaPyr] = 1.5 M	1340	-45	0.7	0.2	0.1

References

1. S. Fujiwara, M. Hosoyamada, K. Tateishi, T. Uesaka, K. Ideta, N. Kimizuka, N. Yanai, Dynamic nuclear polarization of metal-organic frameworks using photoexcited triplet electrons. *J. Am. Chem. Soc.* **140**, 15606-15610 (2018).
2. S. Fujiwara, N. Matsumoto, K. Nishimura, N. Kimizuka, K. Tateishi, T. Uesaka, N. Yanai, Triplet dynamic nuclear polarization of guest molecules through induced fit in a flexible metal-organic framework. *Angew. Chem. Int. Ed. Engl.* **61**, e202115792 (2021).
3. K. Takeda, OPENCORE NMR: Open-source core modules for implementing an integrated FPGA-based NMR spectrometer. *J. Magn. Reson.* **192**, 218-229 (2008).
4. J. Wang, R. M. Wolf, J. W. Caldwell, P. A. Kollman, D. A. Case, Development and testing of a general amber force field. *J. Comput. Chem.* **25**, 1157-1174 (2004).
5. H. W. Horn, W. C. Swope, J. W. Pitera, J. D. Madura, T. J. Dick, G. L. Hura, T. Head-Gordon, Development of an improved four-site water model for biomolecular simulations: TIP4P-Ew. *J. Chem. Phys.* **120**, 9665-9678 (2004).
6. C. I. Bayly, P. Cieplak, W. D. Cornell, P. A. Kollman, A well-behaved electrostatic potential based method using charge restraints for deriving atomic charges - the RESP model. *J. Phys. Chem.* **97**, 10269-10280 (1993).
7. H. J. C. Berendsen, J. P. M. Postma, W. F. Vangunsteren, A. Dinola, J. R. Haak, Molecular-dynamics with coupling to an external bath. *J. Chem. Phys.* **81**, 3684-3690 (1984).
8. S. Nose, A molecular-dynamics method for simulations in the canonical ensemble. *Mol. Phys.* **52**, 255-268 (1984).
9. M. Parrinello, A. Rahman, Polymorphic transitions in single-crystals - A new molecular-dynamics method. *J. Appl. Phys.* **52**, 7182-7190 (1981).
10. B. Hess, H. Bekker, H. J. C. Berendsen, J. Fraaije, LINCS: A linear constraint solver for molecular simulations. *J. Comput. Chem.* **18**, 1463-1472 (1997).
11. T. Darden, D. York, L. Pedersen, Particle mesh Ewald - An *N*.log(*N*) method for Ewald sums in large systems. *J. Chem. Phys.* **98**, 10089-10092 (1993).
12. Henstra, A., Ducksen, P., Schmidt, J. & Wenckebach, W. T. Nuclear Spin Orientation via Electron Spin Locking (NOVEL). *J. Magn. Reson.* **77**, 389-393 (1988).
13. Henstra, A., Schmidt, J., Lin, T.-S. & Wenckebach, W. T. High dynamic nuclear polarization at room temperature. *Chem. Phys. Lett.* **165**, 6-10 (1990).
14. Henstra, A. & Wenckebach, W. T. The theory of nuclear orientation via electron spin locking (NOVEL). *Mol. Phys.* **106**, 859-871, (2008).
15. K. Nishimura, H. Kouno, Y. Kawashima, K. Orihashi, S. Fujiwara, K. Tateishi, T. Uesaka, N. Kimizuka, N. Yanai, Materials chemistry of triplet dynamic nuclear polarization. *Chem. Commun.* **56**, 7217-7232 (2020).